

PROTON DIFFRACTION SCATTERING ON NUCLEI AND NUCLEAR MATTER DISTRIBUTIONS

G.D.Alkhazov, S.L.Belostotsky, A.A.Vorobyov, G.A.Korolev,
D.M.Seliverstov, A.V.Khanzadeev

Introduction

Starting from the well-known Rutherford's experiments with alpha-particle scattering on atomic nuclei, scattering of various particles was widely used for studying nuclear properties. Experiments with fast electrons proved to be especially fruitful for investigation of the charge distributions in nuclei. To study nuclear matter distributions (including protons and neutrons) one has to use strongly interacting probe particles. Protons of relatively low energy were mainly used for this purpose before 1972. Unfortunately, the mechanism of proton scattering on nuclei at low energy is rather complicated, and up to now there is no theory capable to deduce reliable information on nuclear matter distributions from the low energy scattering data. The situation is quite different at higher energy where the scattering is of diffraction nature. The scattering mechanism becomes here quite simple, and it is possible to formulate a diffraction multiple scattering theory which is accurate enough to obtain quantitative information on nuclear matter distributions. The optimum energy of the protons proved to be about 1 GeV. It is just at this energy that various corrections to the multiplescattering theory (theory of Glauber-Sitenko) are small. Also, the spin-spin terms of the proton-nucleon interaction amplitude at small scattering angles are quite small at 1 GeV that facilitates the analysis of the scattering data and reduces uncertainties in the deduced parameters of the density distributions. The first experiments on elastic scattering of high-energy (1 GeV) protons on nuclei ^4He , ^{12}C , and ^{16}O were performed at the Brookhaven National Laboratory by Palevsky et al. in 1967. However, the accuracy of the data obtained was not enough to extract the information on nuclear distributions.

The first high precision measurements of the differential cross sections for elastic scattering of the 1 GeV protons on nuclei were performed at PNPI (LNPI) in 1972. It was demonstrated that with this method one can obtain information on the nuclear matter distributions with the accuracy comparable to that reached in studying nuclear charge distributions by the method of electron elastic scattering. Starting from 1973, similar investigations were performed also at Saclay ($E_p = 1$ GeV) and later (from 1977) at Los Alamos ($E_p = 0.8$ GeV). Thus, the study of diffraction scattering of ~ 1 GeV protons on nuclei became a new branch of experimental research in nuclear physics, and it is due to these studies that the most accurate information on nuclear matter distributions has been obtained by present. Recently, the method of elastic proton-nucleus scattering has been applied in "inverse" kinematics for studying nuclear matter distributions in exotic unstable nuclei.

The proton elastic scattering on nuclei allows to get information on the nuclear matter distributions in the ground nuclear state, while the inelastic scattering makes it possible to study transition nuclear densities. A series of such experiments was performed by the Saclay-PNPI collaboration at the accelerator SATURN at Saclay.

Measurements of differential cross sections

Differential cross sections for elastic and inelastic scattering of protons on stable nuclei are usually measured in "direct" kinematics. Fast protons ($E_p = 1$ GeV in PNPI experiments) are scattered from the target nuclei, the scattering angle being measured. The main problem to be solved in these experiments is selection of the scattering channel. It is not sufficient to measure the scattering angle with relatively high accuracy, but it is also necessary to determine whether it was elastic scattering or inelastic with excitation of some nuclear state. To determine the scattering channel, the energy of the scattered particle is measured. Since the energy of the incident proton is 1 GeV, while the energy loss associated with the nuclear excitations is about 1 MeV or less, a high resolution spectrometer is needed. A magnetic spectrometer with appropriate characteristics has been constructed at PNPI (Fig. 1).

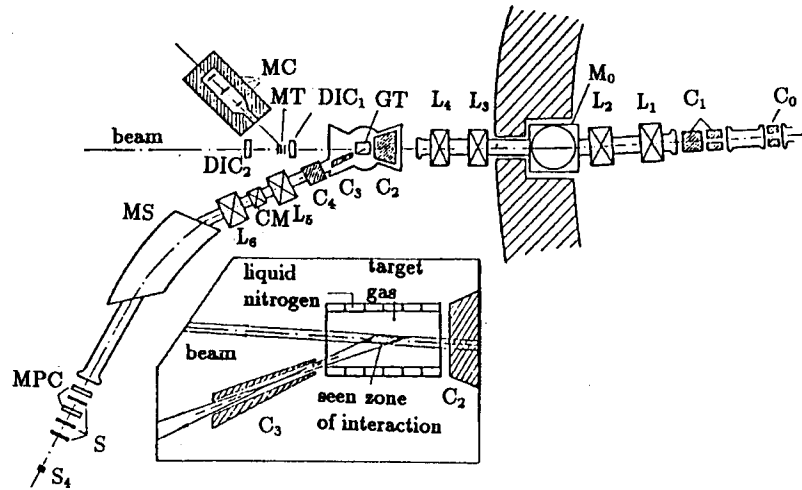


Fig. 1. Schematic layout of the magnetic spectrometer for investigation of elastic and inelastic scattering of 1 GeV protons from nuclei. C_0 – C_4 – collimators, L_1 – L_6 – magnetic quadrupole lenses, M_0 – magnet bending the incident proton beam, MS – the main spectrometer magnet, CM – correcting magnet, S_1 – S_4 – scintillation counters, MPC – multiwire proportional chambers, GM – target with the nuclei under study (gas version of the target is shown), MT – monitor target, DIC₁ and DIC₂ – differential ionization chambers, M – monitor counters.

The energy of the scattered particles is determined by the bending angle in the magnetic spectrometer. The angular focusing is accomplished with two quadrupole lenses and partly with the magnet fringe fields. The total length of the spectrometer from the target to the focal plane, where the scattered particles are registered with the scintillator counters, is about 12 meters. The spectrometer may be rotated around the vertical axis traversing the target. The scattering angle is measured with the accuracy better than 1 mrad. The energy resolution of the spectrometer is $\sim 0.1\%$, that is ~ 1 MeV. Note that using this spectrometer it is possible to separate the scattering channels if the energy of the incident protons is known with sufficient accuracy. However, the energy spread of the proton beam extracted from the PNPI synchrocyclotron is about 10 MeV while the energy gap between the elastic and inelastic scattering channels in the most favorable cases varies from 2 to 4 MeV.

Fortunately, as it has become clear, the energy of the protons in the extracted beam is correlated with their extraction time, the energy being increased from the start to the end of the extraction process. Using this correlation, it became possible to make the proton beam "monochromatic" [1]. The contribution of the energy spread of the extracted beam to the overall resolution of the spectrometer was reduced by this method down to 0.3 MeV without a loss in the intensity of the beam used.

Description of diffraction scattering of 1 GeV protons on nuclei by the theory of multiple scattering

The success of the method of elastic and inelastic scattering of 1 GeV protons on nuclei is to a great extent due to existence at this energy of an accurate theory of scattering that allows to determine quite unambiguously the unknown parameters of nucleon distributions from the measured differential cross sections. Several versions of the multiple scattering theory are used at present for description of diffraction scattering of fast particles on nuclei. These are the theory formulated by Glauber and Sitenko, the theory of Kerman, Mac-Manus and Thaler, and also the relativistic impulse approximation. Note that the Glauber–Sitenko theory was formulated originally only for description of the scattering of fast particles on nuclei at very small angles. Later it was found that the region of the theory applicability is much wider. In particular, it describes the scattering process fairly well in a quite wide angular range. A great number of theoretical papers was devoted to justification of the theory and to the ways of its improvement. It has occurred that the leading correction terms to the basic formula of the Glauber–Sitenko theory (kinematics corrections, non-eikonal corrections, corrections for Fermi-motion) are of about the same magnitude and of different signs, so that when summed up they cancel each other substantially. As a result, the Glauber–Sitenko theory describes the differential cross sections for proton-nucleus scattering with the accuracy not worse than other more sophisticated versions of the multiple scattering theory. According to the Glauber-Sitenko theory, the amplitude of the proton-nucleus scattering is given by the formula

$$F_f(\vec{q}) = (ik/2\pi) \int e^{i\vec{q}\vec{b}} \langle f | 1 - \prod_{j=1}^A [1 - \gamma(\vec{b} - \vec{s}_j)] | i \rangle d^2\vec{b}, \quad (1)$$

where i and f are the initial and final nuclear states, \vec{q} is the momentum transfer, \vec{b} is the impact vector, \vec{s}_j are the transverse nuclear coordinates, k is the magnitude of the wave vector of the incident protons. The proton-nucleon profile function $\gamma_j(\vec{b})$ that enters (1) is connected with the proton-nucleon free scattering amplitude via the relation

$$\gamma_j(\vec{b}) = (1/2\pi ik) \int e^{-i\vec{q}\vec{b}} f_j(\vec{q}) d^2\vec{q}. \quad (2)$$

For small angle proton-nucleus scattering at 1 GeV, the influence of the spin-spin proton-nucleon interaction is small and may be neglected. As for the spin-orbit proton-nucleon interaction, it was studied in our measurements of the polarization in the proton-nucleus scattering at 1 GeV (with a polarimeter in the focal plane of the magnetic spectrometer). Note that the polarization in the elastic proton-nucleus scattering is sensitive to the spin-orbit proton-nucleon interaction. As a result of these measurements it followed that the spin-orbit proton-nucleon interaction at 1 GeV is relatively small, and its influence on the nuclear density parameters

under search is not significant. Thus, the cross sections of the proton-nucleus scattering depend mainly on the nuclear densities and on the scalar proton-nucleon interaction. The amplitude of this interaction was parametrized as

$$f_c(q) = (k\sigma/4\pi)(i + \epsilon_c)\exp(-\beta_c q^2/2), \quad (3)$$

where σ , ϵ_c and β_c are the well-known parameters. The Coulomb interaction gives a relatively small contribution to the cross sections. It was taken into account in a standard way. As it has been shown by the authors [2], the nucleon correlations affect very little the cross sections for proton-nucleus elastic scattering, as well as for scattering with excitation of the lowest 2^+ and 3^- nuclear states, and in the first approximation they may be neglected. Accordingly, the many-body transition density $\rho_{fi}(\vec{r}_1, \vec{r}_2 \dots \vec{r}_A) \equiv \Psi_f^* \Psi_i$ needed for calculation of the amplitude (1) was taken in the form

$$\rho_{ii}(\vec{r}_1, \dots \vec{r}_A) = \prod_{j=1}^A \rho_o(\vec{r}_j) \quad (4)$$

for elastic scattering and

$$\rho_{fi}(\vec{r}_1, \dots \vec{r}_A) = \sum_{j=1}^A \rho_{fi}(\vec{r}_j) \prod_{k \neq j}^A \rho_o(\vec{r}_k) \quad (5)$$

for inelastic scattering, where $\rho_o(\vec{r}_j)$ and $\rho_{fi}(\vec{r}_j)$ are the one-body density of the ground state and the one-body transition density, respectively.

In the analysis performed, the densities $\rho_o(\vec{r}_j)$ were taken as the 3-parameter Fermi distributions

$$\rho_o^{(j)}(\vec{r}) \sim [1 + w_j(r/R_j)^2][1 + \exp((r - R_j)/a_j)]^{-1}. \quad (6)$$

Here $\rho_o^{(j)}(r)$ with $j = p$ or n signify the one-body proton or the one-body neutron densities, respectively.

The one-body transition densities for transitions from the ground 0^+ nuclear state to an excited state with spin L , spin projection M , and parity $(-1)^L$ may be presented as

$$\rho_{fi}(\vec{r}) = \rho_L(r) Y_{LM}^*(\vec{r}/r), \quad (7)$$

where $\rho_L(r)$ is the so-called radial transition density and $Y_{LM}(\vec{r}/r)$ is the spherical harmonic.

The applicability of the Glauber-Sitenko theory for description of the differential cross sections was tested in the case of proton scattering on magic nuclei ^{16}O and ^{40}Ca . According to the nuclear structure theory, the difference between the neutron and proton distributions in these nuclei should be very small. As shown in Ref. [3], the differential cross sections calculated with the Glauber-Sitenko theory for 1 GeV proton elastic scattering, under assumption that the neutron distributions in these nuclei coincide with the proton ones, are in good agreement with the experimental data. The proton distribution parameters used in these calculations were taken from the known data on electron-nucleus scattering.

Fig. 2 shows a comparison between the experimental and theoretical cross sections in the case of ^{40}Ca . One can see that with increasing the scattering angle the cross section decreases by more than 4 orders of magnitude. However, the calculated cross section describes the experimental data perfectly well almost in all this angular range. Note that the calculation is performed without any free parameter! The neutron density distribution found in this way is very close to the proton distribution. The difference between the root-mean square (rms)

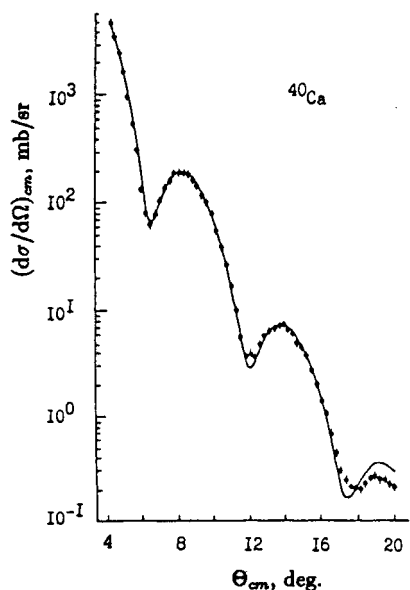


Fig. 2. Differential cross sections for elastic scattering of 1 GeV protons on ^{40}Ca .

Dots – experimental data; solid line – cross section calculated by the Glauber–Sitenko theory without any free parameters, the parameters of the density distributions being taken from the electron scattering experiments.

radii of the neutron and the proton distributions occurred to be zero within the experimental uncertainties (± 0.05 fm). This analysis has demonstrated the applicability of the multiple scattering theory with the approximations used for description of the 1 GeV proton scattering on nuclei.

Elastic proton scattering on nuclei and spatial neutron and nuclear matter distributions

The nucleon spatial distributions in the nuclear ground states as well as the nuclear transition densities are among the basic nuclear characteristics. The experimental information on the nucleon density distributions may be used as a sensitive test of nuclear models.

Investigation of the nucleon distributions in magic nuclei is most important. In our experiments, all the magic nuclei have been investigated [3,4]. The neutron distribution parameters were found from the best fit to the experimental cross sections by the calculated ones (Fig. 3). In these calculations the parameters of the proton distributions were taken from the data on electron-nucleus scattering. As it has been already mentioned, the neutron distributions in ^{16}O and ^{40}Ca were found to be very close to the proton distributions. Similar situation is also in other light nuclei [3,5] (see Table 1). On the other hand, a noticeable difference between the neutron and proton distributions is observed in the nuclei ^{48}Ca and ^{208}Pb (Fig. 4).

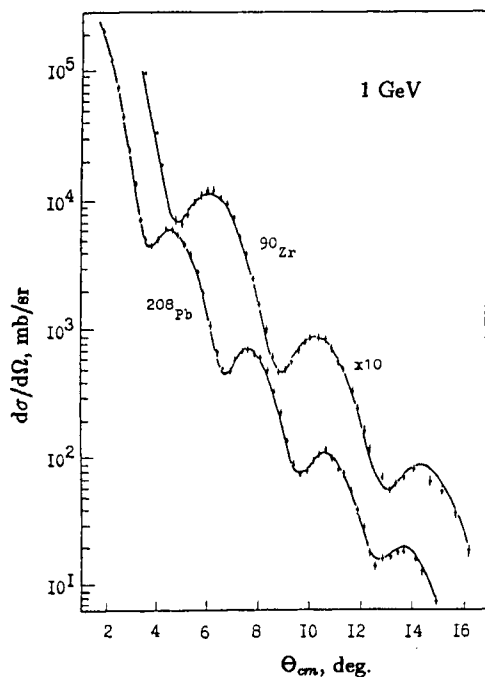


Fig. 3. Differential cross sections for elastic scattering of 1 GeV protons on ^{90}Zr and ^{208}Pb . Dots – experimental data; solid lines – cross sections calculated with the Glauber–Sitenko theory.

Table 1

Nucleus	R_p , fm	a_p , fm	$W_n=W_p$	R_n , fm	a_n	$\langle r^2 \rangle_p^{1/2}$, fm	$\langle r^2 \rangle_n^{1/2}$, fm
^{16}O	2.61	0.51	-0.05	2.48	0.55	2.73	2.74
^{28}Si	3.21	0.57	-0.12	3.13	0.61	3.14	3.15
^{32}S	3.44	0.62	-0.21	3.51	0.61	3.24	3.27
^{39}K	3.74	0.59	-0.20	3.75	0.58	3.41	3.41
^{40}Ca	3.71	0.59	-0.13	3.70	0.59	3.49	3.48
^{48}Ca	3.81	0.53	-0.08	4.06	0.52	3.48	3.64
^{90}Zr	4.86	0.57	-0.09	5.09	0.57	4.26	4.41
^{208}Pb	6.72	0.51	-0.06	6.69	0.57	5.50	5.56

Nuclear surface of ^{48}Ca (at $r > 4$ fm) occurred to be neutron enriched. As for the ^{208}Pb nucleus, a relative surplus of protons on the nuclear surface ($5 < r < 7$ fm) is observed (Fig. 4) that may be a consequence of the Coulomb repulsion in this nucleus. However, with increasing of the radius the proton density decreases faster than the neutron one. As a result, the far nuclear periphery ($r > 7.5$ fm) becomes neutron enriched. For the magic nuclei ^{40}Ca and ^{48}Ca , not much different in the atomic numbers, the difference between the rms neutron radii have been obtained with high precision: $\langle r^2 \rangle_n^{1/2} |_{48} - \langle r^2 \rangle_n^{1/2} |_{40} = 0.15 \pm 0.02$ fm. This result was reproduced in another experiment, performed with the SPES-1 spectrometer at Saclay, this result was reproduced. Later the same value (0.16 ± 0.05 fm) was obtained also by the American physicists at Los Alamos.

The measured cross sections are the effective means of checking the nuclear theory predictions concerning the density distributions. The cross sections calculated with the densities obtained in the theory of finite Fermi systems using the method of partly self-consistent field [6] are in good agreement with the experimental data. At the same time, the cross sections calculated with the densities obtained by the Hartree-Fock method differ significantly from

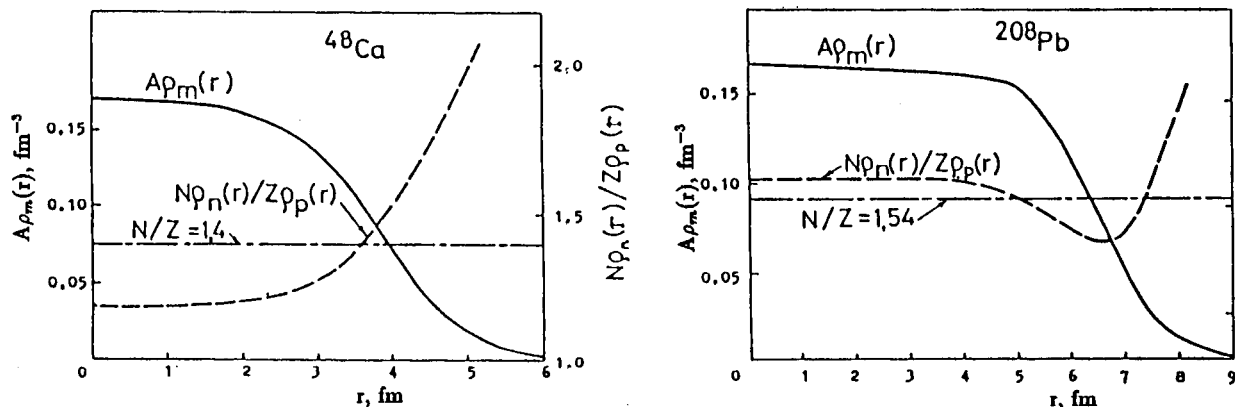


Fig. 4. Radial dependence of the ratio of the neutron density $N\rho_n(r)$ to the proton density $Z\rho_p(r)$ in ^{48}Ca and ^{208}Pb .

the measured ones. The character of the disagreement between the theory and experiment tells us that the theoretical nucleon distributions at the nuclear surface decrease (with the radius increasing) too fast, so that the densities have a reduced surface thickness. Also, the nuclear theories usually (except some latest works) overestimate the difference between the neutron and proton distributions. Note a very good agreement between the calculated and experimental cross sections achieved in the paper of Saperstein and Starodubsky [7], who used a quasi-particle Lagrange method. Having compared the calculated cross sections with the experimental ones, the authors of the mentioned work have excluded the hypothesis of nucleon swelling in nuclei, which was proposed earlier for the explanation of the so-called EMC-effect, and they have obtained a limit on the possible effective increase of the nucleon size in nuclei: $\Delta r_N/r_N \leq 5\%$.

Inelastic scattering of 1 GeV protons and nuclear transition densities

The data on inelastic proton scattering can be used for studying transition nuclear densities which characterize the change of the nuclear density distributions in the transitions from the ground to excited states. Note that not only the neutron transition densities but also the proton ones are studied much less than the ground state densities. A comparison of the calculated and measured cross sections allows to choose the theoretical model that agrees better with the experimental data. Our studies demonstrated that the transition densities of the Bohr-Mottelsson model allow to describe the measured cross sections in a quite satisfactory way, while the popular Tassie model is in a dramatic disagreement with the experimental data (Fig. 5).

The cross sections for inelastic proton-nucleus scattering may be used for determination of some important characteristics of the excited states (namely, for determination of the magnitude and the sign of the nuclear deformation, for clearing out whether the excited nuclear state is of the one-phonon or two-phonon nature).

The analysis of the inelastic scattering of 1 GeV protons from Ni isotopes (these data were obtained in a joint experiment at Saclay) has permitted for the first time to perform a detailed comparison of the isoscalar transition densities with the proton transition densities

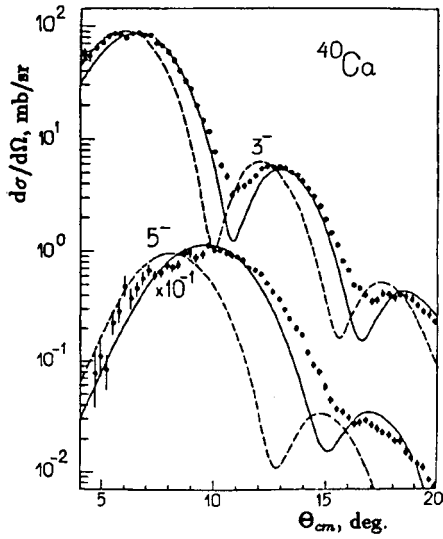


Fig. 5. Differential cross sections for inelastic scattering of 1 GeV protons from ^{40}Ca nuclei. The calculations of the cross sections are performed using the transition densities of the Bohr-Mottelson model (solid lines) and those of the Tassie model (dashed lines). It is seen that the Bohr-Mottelson model is in better agreement with the experiment.

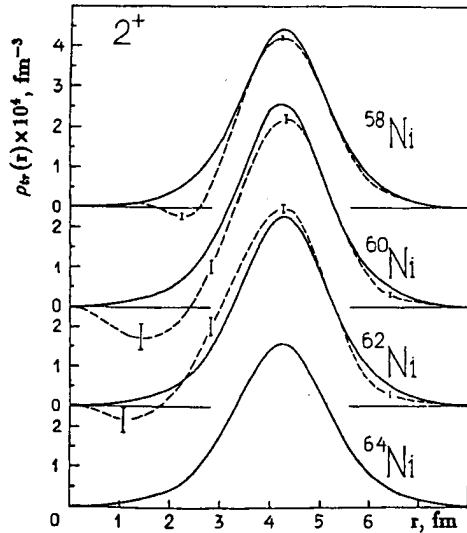


Fig. 6. Comparison of the one-body isoscalar transition densities obtained from the data on inelastic scattering of 1 GeV protons (solid lines) with the charge densities obtained from the data on inelastic scattering of electrons (dashed lines) for $0^+ \rightarrow 2^+$ transitions in Ni isotopes.

for excitation of the lowest $0^+ \rightarrow 2^+$ collective states [8] – see Fig. 6.

The differences between the isoscalar and the proton densities for the transitions considered proved to be small. This result is an evidence for a strong isovector quadrupole polarization of the "core" of the excited nuclei by the valence nucleons. The analysis of the data on 1 GeV inelastic proton-nucleus scattering has allowed also for the first time [8] to compare the isoscalar transition radii with the electromagnetic ones (Fig. 7).

It is seen from Fig. 7 that in the $N = Z$ nuclei the isoscalar transition radius is somewhat smaller than the electromagnetic one though the observed differences are within the error bars. However, in the $N > Z$ nuclei the isoscalar transition radius exceeds systematically the electromagnetic transition radius.

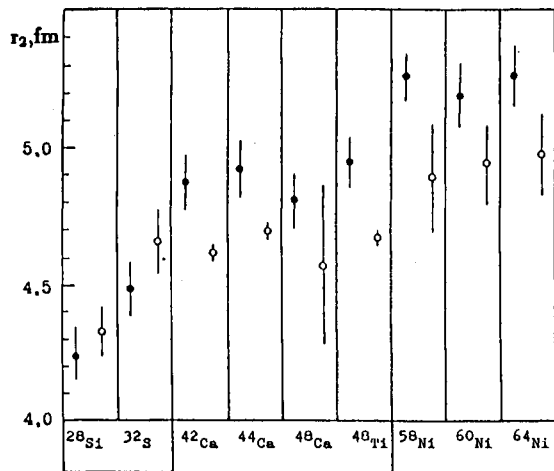


Fig. 7. Comparison of the isoscalar transition radii obtained from the data on proton inelastic scattering (solid circles) with the charge radii obtained from the data on electron scattering (open circles) for $0^+ \rightarrow 2^+$ transitions to the lowest 2^+ states.

Investigation of exotic nuclei by the method of elastic scattering of intermediate energy protons

One of the most interesting events in the recent physics of atomic nuclei was the observation of a neutron halo in the light neutron-rich nuclei such as ^{11}Li or ^{14}Be . As it is established now without any doubts, the structure of these nuclei is considerably different from that of the stable nuclei. These "exotic" nuclei consist of a core with the usual nuclear size and of an extended neutron halo which surrounds the core, the halo size being significantly larger than that of the core. As it has been already discussed here, the most accurate information on the nuclear matter distribution can be obtained from the experiments on elastic scattering of intermediate energy protons. Since it is not possible to use a target of short-lived exotic nuclei, the appropriate experiment can be carried out only in the "inverse" kinematics where a fast beam of exotic nuclei is scattered on a hydrogen target. The intensity of the exotic nuclei beams being relatively low, it is problematic to measure the differential cross sections at large scattering angles with high statistical precision. However, as follows from theoretical considerations, the differential cross sections for elastic scattering even in a limited range of small angles, provided these cross sections are measured with a sufficient precision, allow to obtain information not only on the overall nuclear size but also on the radial distribution of the nuclear matter.

The first experiment on elastic intermediate energy proton scattering from exotic nuclei was performed in a secondary beam of the heavy-ion accelerator at GSI (Darmstadt) with a recoil detector [9] which was developed and constructed at PNPI and was used previously for studies of small angle hadron scattering. In the GSI experiment, we have investigated neutron-rich helium isotopes: ^6He and ^8He . The beams of ^6He and ^8He nuclei with the energy of about 0.7 GeV/nucleon interacted with protons in the hydrogen-filled ionization chamber (IKAR). The hydrogen was the target and the working gas of the ionization chamber. The magnitude of the momentum transfer in the scattering process was determined from the recoil proton energy which was measured with the ionization chamber or from the scattering angle of the projectile (^6He , ^8He) which was measured with multiwire proportional chambers upstream and downstream of IKAR. To check the method, the $p^4\text{He}$ cross section was also measured. The measured cross sections are shown in Fig. 8 as functions of the momentum transfer.

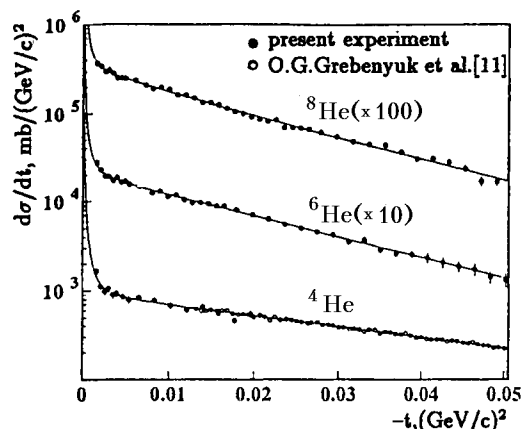


Fig. 8. Differential cross sections for elastic scattering of 0.7 GeV protons from He isotopes, measured in inverse kinematics (solid circles), as functions of the momentum transfer. Open circles are the data of our previous experiment on ${}^4\text{He}$ performed in direct kinematics. Solid lines are cross sections calculated with the Glauber-Sitenko theory.

The cross sections measured in the "inverse" kinematics in case of the $p^4\text{He}$ scattering are in good agreement with our data obtained earlier in the "direct" kinematics [11]. The differential cross sections for elastic scattering of protons from ${}^6\text{He}$ and ${}^8\text{He}$ nuclei have been analyzed with the Glauber-Sitenko theory (Fig. 8). Several two-parameter expressions for description of the nucleon distributions have been used. It occurred that the densities found (Fig. 9) only weakly depend on the particular choice of the density parametrizations (except for the central part of the nucleus and for the far periphery).

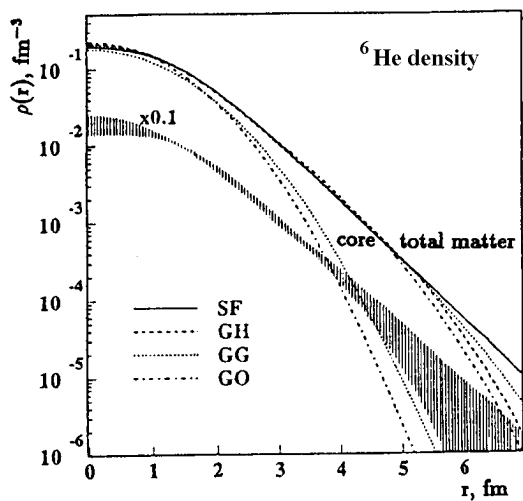


Fig. 9. Nuclear matter distribution in the core and total nucleon distribution in ${}^6\text{He}$ obtained from the data on elastic proton scattering using different nuclear models (SF, GH, GG and GO). The dashed corridor reflects statistical and model uncertainties in the density determination.

The determined root-mean-square radii of the nuclear matter distributions also depend very weakly on the model used and are equal to $R_m = 2.30 \pm 0.10$ fm for ${}^6\text{He}$ and $R_m = 2.45 \pm 0.10$ fm for ${}^8\text{He}$. The results obtained are in agreement with the concept that these nuclei consist of a core with 4 nucleons (the alpha-cluster core) with the radius of 1.6–1.9 fm surrounded by a noticeable neutron "skin" with the thickness of 0.6–1.1 fm. The present experiment has shown that the small-angle elastic scattering of intermediate energy protons in inverse kinematics is an effective means for studying the exotic nuclei. The next stage of the experiment is investigation of heavy Li isotopes, including ${}^{11}\text{Li}$.

References

- [1] *S.L.Belostotsky, G.D.Alkhazov, G.M.Amalsky, A.A.Vorobyov, Yu.V.Dotsenko.* // Pis'ma Zh. Eksp. Teor. Fiz., 1973. V.17. P.101.
- [2] *G.D.Alkhazov, S.L.Belostotsky, A.A.Vorobyov.* // Phys. Reports, 1978. V.42. P.89.
- [3] *G.D.Alkhazov, S.L.Belostotsky, O.A.Domchenkov, Yu.V.Dotsenko, N.P.Kuropatkin, V.N.Nikulin, M.A.Shuvaev, A.A.Vorobyov.* // Nucl. Phys., 1982. V.A381. P.430.
- [4] *G.D.Alkhazov, S.L.Belostotsky, Yu.V.Dotsenko, O.A.Domchenkov, N.P.Kuropatkin, V.N.Nikulin.* // Yad. Fiz., 1985. V.41. P.561.
- [5] *G.D.Alkhazov, S.L.Belostotsky, A.A.Vorobyov, O.A.Domchenkov, Yu.V.Dotsenko, N.P.Kuropatkin, V.N.Nikulin.* // Yad. Fiz., 1985. V.42. P.8.
- [6] *G.D.Alkhazov, B.L.Birbrair, S.I.Glezer, L.P.Lapina, V.A.Sadovnikova.* // Yad. Fiz., 1978. V.27. P.333.
- [7] *E.Ye.Saperstein, V.Ye.Starodubsky.* // Yad. Fiz., 1987. V.46. P.69.
- [8] *G.D.Alkhazov.* // Yad. Fiz., 1988. V.47. P.920.
- [9] *A.A.Vorobyov, G.A.Korolev, V.A.Schegelsky, G.Ye.Solyakin, G.L.Sokolov, Yu.K.Zalite.* // Nucl. Instr. Meth., 1974. V.119. P.509.
- [10] *G.D.Alkhazov, M.N.Andronenko, A.V.Dobrovolsky, G.Ye.Gavrilov, A.V.Khanzadeev, G.A.Korolev, A.A.Lobodenko, D.M.Seliverstov, N.A.Timofeev, A.A.Vorobyov, V.I.Yatsoura et al.* // PNPI Research Report 1994–1995, Gatchina, 1996. P.70.
- [11] *O.G.Grebenyuk, A.V.Khanzadeev, G.A.Korolev, S.I.Manaenkov, J.Saudinos, G.N.Velichko, A.A.Vorobyov.* // Nucl. Phys., 1989. V.A500. P.637.